

Synthesis, X-ray structure, and magnetic properties of interconnected ferromagnetic molecular bowls by hydrogen bonds

Yun Jeong Kim, Eun Young Lee, Mi Young Han, Myunghyun Paik Suh*

School of Chemistry and Molecular Engineering, and Center for Molecular Catalysis, Seoul National University, Seoul 151-747, Republic of Korea

Received 17 April 2003; accepted 11 August 2003

Abstract

Ferromagnetic molecular bowls, $[(\mu_3\text{-OH})\text{Cu}_3(\text{L})]\text{Cl}_{0.5}(\text{ClO}_4)_{4.5}\cdot 1.5\text{H}_2\text{O}$ (**A**), were interconnected by the hydrogen bonding interactions with sodium 1,3,5-benzenetricarboxylate (Na_3BTC), and a dimer of molecular bowl $\{[\text{Cu}_3(\text{L})(\mu_3\text{-OH})_2(\text{C}_9\text{H}_3\text{O}_6)](\text{ClO}_4)_6\cdot \text{Cl}\cdot 8\text{H}_2\text{O}$ (**1**) was isolated. In the structure, two molecular bowls are connected to a BTC^{3-} ion via the μ_3 -hydroxo groups by the hydrogen-bonding interactions, which gives rise to a Y-shaped nano-sized molecule ($12.1 \times 19.1 \times 19.9 \text{ \AA}^3$). Each molecular bowl in **1** shows similar bond distances and angles to those of **A**, especially around the Cu^{II} ions and the central oxygen atom. Variable temperature magnetic susceptibility data indicate that compound **1** has magnetic parameters of $g = 2.03$, $J = 37.8 \text{ cm}^{-1}$ and $zJ' = -0.50 \text{ cm}^{-1}$ and $R = 1.54 \times 10^{-5}$. Three $\text{Cu}(\text{II})$ ions within a molecular bowl exhibit relatively strong ferromagnetic interaction, but a weak antiferromagnetic interaction occurs between the two Cu_3 units connected to a BTC^{3-} .
© 2003 Elsevier B.V. All rights reserved.

Keywords: Copper complexes; Ferromagnetic interactions; Hydrogen bonds; Molecular bowls

1. Introduction

Big molecules with multi-paramagnetic metal centers have attracted considerable attention due to their interesting structures as well as potential applications as nanoscale molecular devices [1] and new inorganic magnetic materials [2]. In the design of nano-sized molecules, hydrogen bonding has been extensively employed to connect smaller molecular units [3]. Furthermore, hydrogen bond often offers the path for magnetic coupling between the paramagnetic metal centers. For example, $\text{Fe}(\text{III})$ complexes such as $[\text{Fe}(\text{bipym})\text{Cl}_3(\text{H}_2\text{O})]\cdot \text{H}_2\text{O}$ and $[\text{Fe}_2(\text{bipym})\text{Cl}_6(\text{H}_2\text{O})_2]\cdot (\text{H}_2\text{O})_2$ (bipym = 2,2'-bipyrimidine) show antiferromagnetic coupling between the intermolecular $\text{Fe}(\text{III})$ ions that are connected by the hydrogen bonding interactions via the coordinated water molecules and the chlorine atoms of the neighboring complexes [4]. The complexes $[\text{Ni}(\text{L}_n)_2(\text{CH}_3\text{OH})_2]$, $[\text{Ni}(\text{L}_n)_2(\text{C}_2\text{H}_5\text{OH})_2]$, and

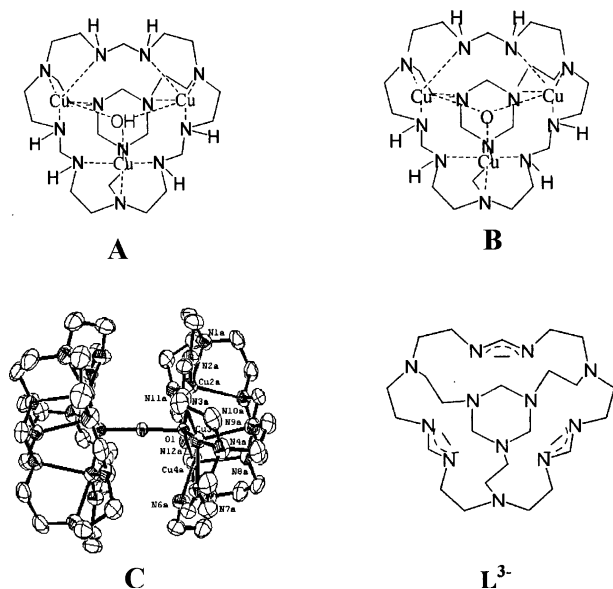
$[\text{Ni}(\text{L}_n)_2(\text{OH}(\text{CH}_2)_5\text{OH})]$ (L_n = a deprotonated nitroxide 4-(3',3',3'-trifluoromethyl-2'-oxo-propylidene)-2,2,5,5-tetramethyl-3-imidazoline-1-oxyl) form 2D layers due to the hydrogen bonding interactions, and they show weak ferromagnetic interactions between the $\text{Ni}(\text{II})$ ions [5]. The complex $[\text{Fe}(\text{CN})_6]_2[\text{Ni}(\text{bpm})_2]_3(\text{H}_2\text{O})_7$ (bpm = bis(1-pyrazolyl)methane) shows uncommon magnetic behavior, in which $\chi_M T$ values are significantly greater than the values expected for an isolated $S = 4$ of $\text{Fe}_2^{\text{III}}\text{Ni}_3^{\text{II}}$ cluster, because three dimensional magnetic ordering is induced by the hydrogen bonding interactions [6].

Previously, we have prepared molecular bowls with μ_3 -hydroxo and μ_3 -oxo tricopper(II) cores, $[(\mu_3\text{-OH})\text{Cu}_3(\text{L})](\text{ClO}_4)_{4.5}\cdot \text{Cl}_{0.5}\cdot 1.5\text{H}_2\text{O}$ (**A**) and $[(\mu_3\text{-O})\text{Cu}_3(\text{L})](\text{ClO}_4)_4\cdot 2\text{H}_2\text{O}$ (**B**), respectively, by the one-pot template condensation reaction of tris(2-aminoethyl)amine and formaldehyde in the presence of Cu^{II} ion [7]. The compounds exhibit unusually strong ferromagnetic interactions between the three Cu^{II} ions with $J = 37.8 \text{ cm}^{-1}$ for **A** and $J = 109 \text{ cm}^{-1}$ for **B** on the basis of $H = -J(S_1\cdot S_2 + S_2\cdot S_3 + S_3\cdot S_1) - g\mu_B(S_1 + S_2 + S_3)\cdot H$. In addition, we have prepared a molecular dumbbell $\text{Cu}^{\text{I}}[(\mu_4\text{-O})\text{Cu}_3^{\text{II}}(\text{L}^{3-})_2](\text{ClO}_4)_3\cdot \text{MeCOMe}$ (**C**), in which

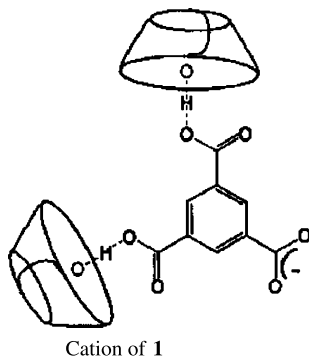
* Corresponding author. Tel.: +82-2-880-7760; fax: +82-2-886-8516.

E-mail address: mpsuh@snu.ac.kr (M.P. Suh).

two molecular bowls (**B**) are interconnected in a face to face mode by a Cu^{I} metal bridge [8]. Contrary to the molecular bowls, the molecular dumbbell **C** shows strong antiferromagnetism ($J = -129 \text{ cm}^{-1}$). The X-ray crystal structure of the molecular dumbbell indicates that the $\text{Cu}^{\text{II}}\text{--O}$ bond distances and $\text{Cu}^{\text{II}}\text{--O--Cu}^{\text{II}}$ bond angles are increased compared with those of the molecular bowls, which causes the dramatic change of magnetic property.



To obtain bigger molecules containing more paramagnetic metal centers and to see the effect of hydrogen bonds on the magnetic couplings, we interconnected the molecular bowls **A** with sodium 1,3,5-benzenetricarboxylate. In this paper, we report the synthesis, X-ray structure and magnetic property of $\{[\text{Cu}_3(\text{L})(\mu_3\text{-OH})]_2(\text{C}_9\text{H}_3\text{O}_6)\}(\text{ClO}_4)_6 \cdot \text{Cl} \cdot 8\text{H}_2\text{O}$ (**1**).



2. Experimental

2.1. Materials

All chemicals used in the synthesis were of reagent grade and were used without further purification. For

the spectroscopic and electrochemical measurements, solvents were purified according to the literature [9]. Compound **A** was prepared according to the literature published previously [7].

2.2. Measurements

Infrared spectrum was recorded with a Perkin Elmer 2000 FT-IR spectrophotometer. Electronic absorption spectrum was obtained on a Cary 300 Bio UV–vis spectrophotometer. Magnetic susceptibility was measured on a Quantum Design MPMS superconducting quantum interference device (SQUID) at Korea Basic Science Institute, Deajeon. Elemental analysis was performed by the analytical laboratory in Seoul National University.

2.3. Syntheses

Safety note: caution. Perchlorate salts of metal complexes with organic ligands are potentially explosive. Only small amounts of material should be prepared and these should be handled with great care.

2.3.1. $\{[\text{Cu}_3(\text{L})(\mu_3\text{-OH})]_2(\text{C}_9\text{H}_3\text{O}_6)\}(\text{ClO}_4)_6 \cdot \text{Cl} \cdot 8\text{H}_2\text{O}$ (**1**)

$[\text{Cu}_3(\text{L})(\mu_3\text{-OH})](\text{ClO}_4)_{4.5} \cdot \text{Cl}_{0.5} \cdot 1.5\text{H}_2\text{O}$ (**A**) (2.00 g, 1.652 mmol) was dissolved in the mixture of MeOH and H_2O (1:1 v/v, 70 ml) at the elevated temperature, and then the MeOH– H_2O solution (1:1 v/v, 10 ml) of sodium 1,3,5-benzenetricarboxylate (0.400 g, 1.449 mmol) was added dropwise. The solution was allowed to stand at room temperature for ca. 24 h until blue–green precipitate formed, which was filtered off, washed with acetone, and dried in air. Yield: 77%. The product was recrystallized from hot water (75 ml) and bluish green crystals formed, which were filtered, washed with acetone, and dried in air. *Anal.* Calc. for $\text{Cu}_6\text{C}_{57}\text{H}_{129}\text{N}_{24}\text{Cl}_7\text{O}_{40}$: C, 28.29; H, 5.37; N, 13.89%. Found: C, 28.20; H, 4.29; N, 13.90%. FT-IR (Nujol mull): $\nu_{\text{O=C-O}^-}$, 1605 cm^{-1} ; $\nu_{\text{C=C}}$, 1558 cm^{-1} ; $\nu_{\text{H}_2\text{O}}$, $3591, 3350, 3204 \text{ cm}^{-1}$; $\nu_{\text{O-H}\cdots\text{O}}$, $2162, 2028$; $\nu_{\text{N-H}}$, 3114 cm^{-1} . UV–vis (in H_2O), λ_{max} (ϵ , $\text{M}^{-1} \text{ cm}^{-1}$): 657 nm (1130), 753 nm (1110).

2.4. X-ray diffraction measurement for $\{[\text{Cu}_3(\text{L})(\mu_3\text{-OH})]_2(\text{C}_9\text{H}_3\text{O}_6)\}(\text{ClO}_4)_6 \cdot \text{Cl} \cdot 8\text{H}_2\text{O}$ (**1**)

X-ray examination and data collection procedures for a single crystal **1** ($0.20 \times 0.30 \times 0.50 \text{ mm}^3$) were performed with an Enraf Nonius kappa CCD diffractometer (Mo $\text{K}\alpha$, $\lambda = 0.71073 \text{ \AA}$, graphite monochromator). Preliminary orientation matrices and unit cell parameters were obtained from the peaks of the

first ten frames and were then refined using the whole data set. Frames were integrated and corrected for Lorentz and polarization effects using DENZO [10]. The scaling and the global refinement of crystal parameters were performed by SCALEPACK [10]. No absorption correction was made. The crystal structure was solved by the direct method [11] and refined by full-matrix least-squares refinement using the SHELXL-97 computer program [12]. The positions of all non-hydrogen atoms were refined with anisotropic displacement factors. The hydrogen atoms were positioned geometrically and refined using a riding model. The distances between each μ_3 -oxygen atom and the corresponding oxygen atom of BTC^{3-} is 2.513(7) Å for $\text{Cu}_3(\text{a})$ and 2.514(7) Å for $\text{Cu}_3(\text{b})$, which indicate the existence of hydrogen bonds between them, but the hydrogen atoms involving the hydrogen bonds were not detected from the Fourier map. The crystallographic data of **1** are summarized in Table 1.

Table 1
Crystallographic data for $\{[\text{Cu}_3(\text{L})(\mu_3\text{-OH})]_2(\text{C}_9\text{H}_3\text{O}_6)\}(\text{ClO}_4)_6 \cdot \text{Cl} \cdot 8\text{H}_2\text{O}$ (**1**)

Formula	$\text{Cu}_6\text{C}_{57}\text{N}_{24}\text{H}_{129}\text{O}_{40}\text{Cl}_7$
F_w	2420.29
T (K)	293(2)
λ (Å)	0.71073
Crystal system	triclinic
Space group	$P\bar{1}$
Unit cell dimensions	
a (Å)	12.124
b (Å)	19.6550(10)
c (Å)	19.912
α (°)	95.702(2)
β (°)	101.468(2)
γ (°)	90.2090(10)
V (Å ³)	4625.9(2)
Z	2
D_{calc} (g cm ⁻³)	1.738
Absorption coefficient (mm ⁻¹)	1.657
$F(000)$	2504
Crystal size (mm ³)	0.50 × 0.40 × 0.20
θ Range for data collection (°)	1.55–27.46
Index ranges	–14 ≤ h ≤ 15, –25 ≤ k ≤ 23, –25 ≤ l ≤ 25
Reflections collected	32340
Independent reflections	20520 [$R_{\text{int}} = 0.0417$]
Completeness to $\theta = 27.46$ (%)	96.9
Refinement method	full-matrix least-squares on F^2
Data/restraints/parameters	20520/0/1170
Goodness-of-fit on F^2	1.043
Final R indices [$I > 2\sigma(I)$] ^a	$R_1 = 0.1034$, $wR_2 = 0.2555$
R indices (all data) ^a	$R_1 = 0.1485$, $wR_2 = 0.3000$
Largest difference peak and hole (e Å ⁻³)	2.726 and –1.939

^a $R = \sum ||F_o| - |F_c|| / \sum |F_o|$, $wR(F^2) = [\sum w(F_o^2 - F_c^2)^2 / \sum w(F_o^2)^2]^{1/2}$
where $w = 1/[\sigma^2(F_o^2) + (0.1427P)^2 + (47.80)P]$, $P = (\max(F_o^2, 0) + 2F_c^2)/3$.

3. Results and discussion

3.1. Synthesis of interconnected ferromagnetic molecular bowls by hydrogen bonding

Since the crystal structure of parent $[(\mu_3\text{-OH})\text{Cu}_3(\text{L})](\text{ClO}_4)_{4.5} \cdot \text{Cl}_{0.5} \cdot 1.5\text{H}_2\text{O}$ (**A**) shows hydrogen bonding interaction between $\mu_3\text{-OH}$ group and Cl^- anion [7], we expected that several units of μ_3 -hydroxo molecular bowls may be interconnected by the hydrogen bonding interactions with tricarboxylate anion.

The μ_3 -hydroxo molecular bowls (**A**) were interconnected by the hydrogen bonding with 1,3,5-benzenetricarboxylate anion, which resulted in **1**. Although we expected that three molecular bowls can be linked by a BTC^{3-} ion, the trimer was never obtained probably due to the steric hindrance between them.

3.2. X-ray crystal structure and property of $\{[\text{Cu}_3(\text{L})(\mu_3\text{-OH})]_2(\text{C}_9\text{H}_3\text{O}_6)\}(\text{ClO}_4)_6 \cdot \text{Cl} \cdot 8\text{H}_2\text{O}$ (**1**)

The view of the cation in **1** is shown in Fig. 1 [13]. Table 2 shows the selected bond distances and angles. In the structure, two molecular bowls are linked to a BTC^{3-} ion by hydrogen-bonds via the μ_3 -hydroxo groups, which gives rise to a Y-shaped molecule of size $12.1 \times 19.7 \times 19.9$ Å³. Each unit of molecular bowl has similar bond distances and angles to those of **A** [7], especially around three Cu^{II} ions and the central oxygen. Two hydrogen-bond distances, $\text{O}(\mu_3\text{-hydroxo}) \cdots \text{O}(\text{BTC}^{3-})$ in the $\text{Cu}_3(\text{a})$ and $\text{Cu}_3(\text{b})$ units, are 2.514(7) Å and 2.515(7) Å, respectively. The three Cu^{II} ions locate at the corners of a triangle of side av. 3.250(1) Å in the $\text{Cu}_3(\text{a})$ unit and av. 3.240(1) Å in the $\text{Cu}_3(\text{b})$ unit. The μ_3 -oxygen atoms are positioned 0.555(5) Å and 0.565(5) Å above the plane made by three Cu^{II} ions for the $\text{Cu}_3(\text{a})$ and $\text{Cu}_3(\text{b})$ units, respectively. The angles of $\text{Cu}^{\text{II}}\text{--O--Cu}^{\text{II}}$ are av. 112.3(1)° for $\text{Cu}_3(\text{a})$ and av. 112.0(1)° for $\text{Cu}_3(\text{b})$, which are similar to those of **A**. Each $\text{Cu}(\text{II})$ ion adapts a distorted trigonal bipyramidal coordination geometry by binding two tertiary nitrogen atoms as well as two secondary nitrogen atoms and an oxygen atom. The apical sites are occupied by a μ_3 -oxygen atom and a tertiary nitrogen donor belonging to the larger rim of the bowl. The $\text{N}_{\text{eq}}\text{--Cu}^{\text{II}}\text{--N}_{\text{eq}}$ and $\text{N}_{\text{ax}}\text{--Cu}^{\text{II}}\text{--N}_{\text{eq}}$ bond angles, respectively, are av. 116.1(2)° and av. 84.5(1)° for $\text{Cu}_3(\text{a})$ and av. 121.5(2)° and av. 84.3(1)° for $\text{Cu}_3(\text{b})$. The axial bond distances of $\text{Cu}^{\text{II}}\text{--O}$ and $\text{Cu}^{\text{II}}\text{--N}_{\text{ax}}$, respectively, are av. 1.956(3) Å and av. 2.032(4) Å for $\text{Cu}_3(\text{a})$ and av. 1.954(3) Å and av. 2.039(4) Å for $\text{Cu}_3(\text{b})$. The $\text{Cu}^{\text{II}}\text{--O}$ bond distance is similar to that [av. 1.959(2) Å] of **A**. In the trigonal plane, the $\text{Cu}^{\text{II}}\text{--N}$ bond distances are average 2.163(3) Å for $\text{Cu}_3(\text{a})$ and 2.164(3) Å for $\text{Cu}_3(\text{b})$. The $\text{Cu}(\text{II})$ atom is displaced from the trigonal

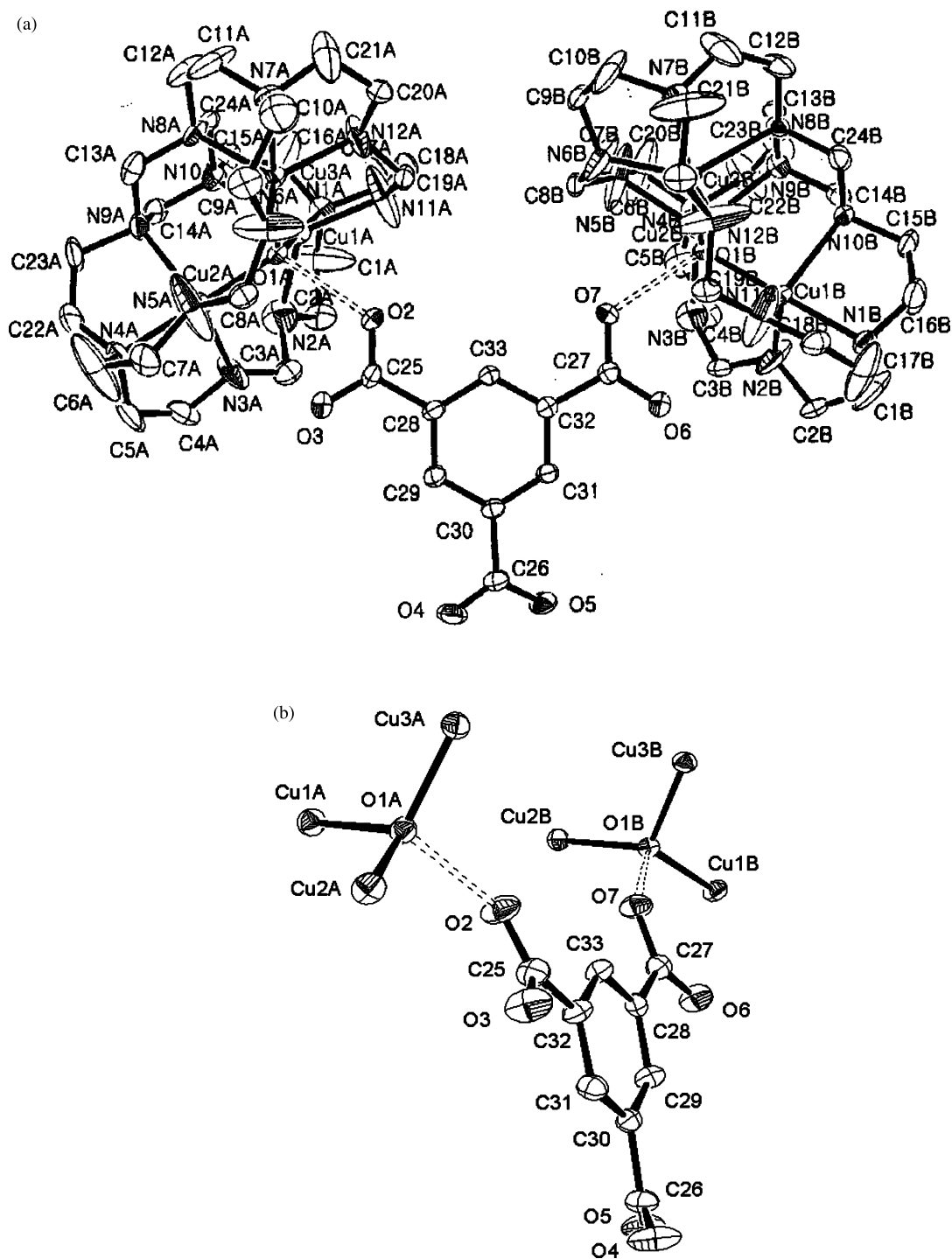


Fig. 1. (a) An ORTEP drawing of compound **1**. The atoms are represented by 40% probable thermal ellipsoid. (b) The core of two trinuclear units interconnected by a BTC³⁻.

plane toward the oxygen atom of BTC³⁻ by av. 0.207(3) Å for Cu₃(a) and av. 0.212(3) Å for Cu₃(b).

The compound **1** is soluble in Me₂SO, DMF, MeCN, MeOH and water, but insoluble in acetone and Et₂O. It is blue–green, similarly to the molecular bowl A. The UV–vis spectrum measured for the aqueous solution of **1** shows a maximum absorption at 657 nm ($\epsilon = 1130$

M⁻¹ cm⁻¹) and 753 nm ($\epsilon = 1110$ M⁻¹ cm⁻¹), indicating that the μ_3 -hydroxo molecular bowls are dissociated from BTC³⁻ in water.

Variable-temperature (2–300 K) magnetic susceptibility data of **1** were measured and the plots of χ_M versus T and $\chi_M T$ versus T are presented in Fig. 2. The value of $\chi_M T$ increases with decreasing temperature

Table 2

Selected bond lengths (Å) and bond angles (°) for $\{[\text{Cu}_3(\text{L})(\mu_3\text{-OH})_2(\text{C}_9\text{H}_5\text{O}_6)](\text{ClO}_4)_6 \cdot \text{Cl} \cdot 8\text{H}_2\text{O} (\mathbf{1})\}$

Bond lengths			
Cu1A–O1A	1.959(5)	Cu1B–O1B	1.952(5)
Cu1A–N1A	2.026(7)	Cu1B–N1B	2.040(7)
Cu1A–N11A	2.032(10)	Cu1B–N11B	2.078(9)
Cu1A–N2A	2.144(13)	Cu1B–N2B	2.089(10)
Cu1A–N10A	2.244(7)	Cu1B–N10B	2.265(7)
Cu2A–O1A	1.949(5)	Cu2B–O1B	1.958(5)
Cu2A–N4A	2.036(7)	Cu2B–N4B	2.041(6)
Cu2A–N3A	2.062(9)	Cu2B–N3B	2.052(10)
Cu2A–N5A	2.066(12)	Cu2B–N5B	2.090(10)
Cu2A–N9A	2.250(7)	Cu2B–N9B	2.233(7)
Cu3A–O1A	1.961(5)	Cu3B–O1B	1.954(5)
Cu3A–N7A	2.035(7)	Cu3B–N7B	2.035(6)
Cu3A–N6A	2.037(10)	Cu3B–N6B	2.036(9)
Cu3A–N12A	2.120(12)	Cu3B–N12B	2.122(10)
Cu3A–N8A	2.233(6)	Cu3B–N8B	2.245(6)
Bond angles			
O1A–Cu1A–N1A	178.7(3)	N1A–Cu1A–N10A	85.6(3)
O1A–Cu1A–N11A	95.8(3)	N11A–Cu1A–N10A	125.5(6)
N1A–Cu1A–N11A	83.8(4)	N2A–Cu1A–N10A	103.0(4)
O1A–Cu1A–N2A	98.0(4)	O1A–Cu2A–N4A	179.0(3)
N1A–Cu1A–N2A	83.2(4)	O1A–Cu2A–N3A	96.3(3)
N11A–Cu1A–N2A	128.3(7)	N4A–Cu2A–N3A	84.0(4)
O1A–Cu1A–N10A	93.6(2)	O1A–Cu2A–N5A	95.5(3)
N4A–Cu2A–N5A	85.1(4)	N1B–Cu1B–N2B	85.0(3)
N3A–Cu2A–N5A	126.8(8)	N11B–Cu1B–N2B	125.3(8)
O1A–Cu2A–N9A	94.0(2)	O1B–Cu1B–N10B	94.4(2)
N4A–Cu2A–N9A	85.0(3)	N1B–Cu1B–N10B	84.9(3)
N3A–Cu2A–N9A	121.1(6)	N11B–Cu1B–N10B	123.1(6)
N5A–Cu2A–N9A	109.5(7)	N2B–Cu1B–N10B	108.8(6)
O1A–Cu3A–N7A	179.3(3)	O1B–Cu2B–N4B	179.6(3)
O1A–Cu3A–N6A	95.5(3)	O1B–Cu2B–N3B	95.3(3)
N7A–Cu3A–N6A	84.1(4)	N4B–Cu2B–N3B	84.4(3)
O1A–Cu3A–N12A	97.1(3)	O1B–Cu2B–N5B	96.7(3)
N7A–Cu3A–N12A	83.6(3)	N4B–Cu2B–N5B	83.5(3)
N6A–Cu3A–N12A	123.8(8)	N3B–Cu2B–N5B	118.0(6)
O1A–Cu3A–N8A	94.7(2)	O1B–Cu2B–N9B	95.1(2)
N7A–Cu3A–N8A	85.2(3)	N4B–Cu2B–N9B	85.1(3)
N6A–Cu3A–N8A	127.1(6)	N3B–Cu2B–N9B	130.1(3)
N12A–Cu3A–N8A	106.1(6)	N5B–Cu2B–N9B	109.0(6)
Cu2A–O1A–Cu1A	112.4(2)	O1B–Cu3B–N7B	178.9(2)
Cu2A–O1A–Cu3A	112.9(2)	O1B–Cu3B–N6B	95.4(3)
Cu1A–O1A–Cu3A	111.6(2)	N7B–Cu3B–N6B	83.9(3)
O1B–Cu1B–N1B	179.3(3)	O1B–Cu3B–N12B	98.1(3)
O1B–Cu1B–N11B	96.5(3)	N7B–Cu3B–N12B	82.9(3)
N1B–Cu1B–N11B	83.6(3)	N6B–Cu3B–N12B	124.8(8)
O1B–Cu1B–N2B	95.5(3)	O1B–Cu3B–N8B	94.5(2)
N7B–Cu3B–N8B	85.3(3)	N6B–Cu3B–N8B	124.7(6)
N12B–Cu3B–N8B	107.3(6)	Cu1B–O1B–Cu2B	112.6(2)
Cu1B–O1B–Cu3B	111.6(2)	Cu3B–O1B–Cu2B	111.8(2)

until it reaches a maximum, indicating a dominant ferromagnetic coupling between the Cu_3 units. At lower temperature, $\chi_{\text{M}}T$ decreases rapidly showing the anti-ferromagnetic coupling, which is ascribed to the interaction between the trimetallic units that are interconnected through BTC^{3-} by the hydrogen bonding interactions.¹ The magnetic data are interpreted in terms of spin Hamiltonian for a Cu_3 unit as described in

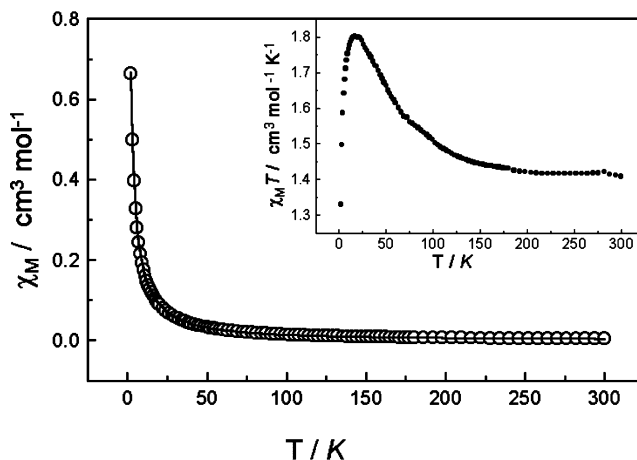


Fig. 2. Plot of χ_{M} vs. T and $\chi_{\text{M}}T$ vs. T (inset) for $\mathbf{1}$ (\circ) under 5000 G. The solid line is the best-fit curve to Eq. (2).

Eq. (1). χ_{M} per trinuclear cluster is expressed as Eq. (2) where $F(T) = (e^{-3/2J/kT} + 5)/(e^{-3/2J/kT} + 1)$ when an intercluster interaction (zJ') through hydrogen bonding is introduced [14–16].²

$$H = -J(S_1S_2 + S_2S_3 + S_3S_1) - g\mu_{\text{B}}(S_1 + S_2 + S_3)H \quad (1)$$

$$\chi_{\text{M}} = Ng^2\mu_{\text{B}}^2 F(T)/[4kT - zJ'F(T)] \quad (2)$$

The best fit parameters for the magnetic susceptibility data to Eq. (2), when tip value for the three copper ions is fixed as $1.8 \times 10^{-4} \text{ cm}^3 \text{ mol}^{-1}$, are $g = 2.03$, $J = 37.8 \text{ cm}^{-1}$, $zJ' = -0.50 \text{ cm}^{-1}$ and $R = 1.54 \times 10^{-5}$ ($R = \text{agreement factor defined as } \Sigma[(\chi_{\text{M}})_{\text{obs}} - (\chi_{\text{M}})_{\text{calc}}]^2 / \Sigma[(\chi_{\text{M}})_{\text{obs}}]^2$). Within a molecular bowl in $\mathbf{1}$, three $\text{Cu}(\text{II})$ ions exhibit relatively strong ferromagnetic interactions with J value same as that (37.8 cm^{-1}) of \mathbf{A} , which must be attributed to their similar structures within the molecular bowl unit (Table 3). Between the two Cu_3 units connected by BTC^{3-} , a weak antiferromagnetic interaction occurs with zJ' value of -0.50 cm^{-1} , probably because the distance between the two Cu_3 unit is too long to have strong magnetic interaction.

Table 3

Comparison of structure and magnetism of $\mathbf{1}$ and with those of \mathbf{A} – \mathbf{C}

Compound	$\text{Cu}^{\text{II}}\text{--O}$ (Å)	$\text{Cu}^{\text{II}}\text{--O--Cu}^{\text{II}}$ (°)	$\text{Cu}^{\text{II}}\cdots\text{Cu}^{\text{II}}$ (Å)	Magnetism, J (cm^{-1})
1	1.956(2)	112.2(1)	3.245(1)	+37.8
A ^a	1.959(2)	112.5(1)	3.258(1)	+37.8
B ^a	1.876(2)	112.3(1)	3.115(1)	+109
C ^b	1.956(2)	114.5(1)	3.290(1)	–125

^a Ref. [7].

^b Ref. [8].

¹ The thermal depopulation of low-lying Zeeman levels may be an alternative or additional reason for the turnover in $\chi_{\text{M}}T$ at low temperature.

² The data were corrected for diamagnetic contribution.

In short, the magnetic interaction in **1** is dominated by the interaction between the Cu(II) ions within a molecular bowl unit. For other $\text{Cu}_3(\mu_3\text{-OH})$ species whose magnetic orbital is $d_{x^2-y^2}$ and Cu–O–Cu bridging angle ranges $106\text{--}109^\circ$, antiferromagnetism was observed [17]. However, the present complex **1** as well as **A** and **B** utilize d_{z^2} orbital as the magnetic orbital and have more flattened Cu–O–Cu angles ($111.6\text{--}112.9^\circ$) to show ferromagnetism. As shown in Table 3, magnetic interactions are much stronger in the μ_3 -oxo complex (**B**), which has shorter Cu–O bond distance, than in the μ_3 -hydroxo complex (**A**) [7]. For the molecular dumbbell (**C**), the Cu^{II}–O bond distances and the Cu^{II}–O–Cu^{II} bond angles are increased compared with those of **A** and **B**, which change the magnetic property to antiferromagnetism [8]. We assume that Cu–O bond distance and the Cu–O–Cu angle determine the ferromagnetism or antiferromagnetism for our compounds containing tricopper molecular bowl unit. It has been reported for the dibridged Cu(II) dimers that the bridging angle is the critical parameter to determine the magnetism; a change of 1° results in a variation of J value ca. 74 cm^{-1} [18].

4. Supplementary material

Crystallographic data for the structural analysis have been deposited with the Cambridge Crystallographic Data Centre, CCDC No. 203309 for compound **1**. Copies of this information may be obtained free of charge from The Director, CCDC, 12 Union Road, Cambridge, CB2 1EZ, UK (fax: +44-1223-336-033; e-mail: deposit@ccdc.cam.ac.uk or www: http://www.ccdc.cam.ac.uk).

Acknowledgements

This work was supported by Korea Institute of S & T Evaluation and Planning (project no. M1-0213-03-0001).

References

- [1] (a) L.F. Lindoy, *Nature* 364 (1993) 17;
(b) P. Ball, *Nature* 362 (1993) 123.
- [2] (a) O. Kahn, C.J. Martinez, *Science* 279 (1998) 44;
(b) O. Kahn, *Molecular Magnetism*, VCH Publishers, New York, 1993.
- [3] (a) D. Braga, L. Maini, F. Grepioni, *Angew. Chem. Int. Ed. Engl.* 37 (1988) 2240;
(b) D. Venkataraman, S. Lee, J. Shang, J.S. Moore, *Nature* 371 (1988) 591;
(c) C. Aakeroy, A.M. Beatty, *J. Chem. Soc. Chem. Commun.* (1988) 1067;
(d) K. Kobayashi, M. Koyanagi, K. Endo, H. Masuda, Y. Aoyama, *Chem. Eur. J.* 4 (1998) 417;
(e) M.J. Zaworotko, *Nature* 386 (1997) 220.
- [4] G. De Munno, W. Ventura, G. Viau, F. Lloret, J. Faus, M. Julve, *Inorg. Chem.* 37 (1998) 1458.
- [5] V.N. Ikorskii, V.I. Ovcharenko, Y.G. Schvedenkov, G.V. Romanenko, S.V. Kokin, R.Z. Sagdeev, *Inorg. Chem.* 37 (1998) 4360.
- [6] K.V. Langenberg, S.R. Batten, K.J. Berry, D.C.R. Hockless, B. Moubaraki, K.S. Murray, *Inorg. Chem.* 36 (1997) 5006.
- [7] M.P. Suh, M.Y. Han, J.H. Lee, K.S. Min, C. Hyeon, *J. Am. Chem. Soc.* 120 (1998) 3819.
- [8] M.Y. Han, K.S. Min, M.P. Suh, *Inorg. Chem.* 38 (1999) 4374.
- [9] D.D. Perrin, W.L.F. Armarego, *Purification of Laboratory Chemicals*, 3rd ed., Pergamon Press, Oxford, UK, 1988.
- [10] Z. Otwinowsky, W. Minor, *Processing of X-ray diffraction data collected in oscillation mode*, in: C.W. Carter, Jr, R.M. Sweet (Eds.), *Methods in Enzymology*, vol. 276, Academic Press, New York, 1996, pp. 307–326.
- [11] G.M. Sheldrick, *Acta Crystallogr.* A46 (1990) 467.
- [12] G.M. Sheldrick, *SHELXL-97*, Program for the Crystal Structure Refinement, University of Göttingen, Göttingen, Germany, 1997.
- [13] L.J. Farrugia, *ORTEP-3 for Windows*, Version 1.02 Beta, University of Glasgow, Glasgow, Scotland, UK, 1997.
- [14] (a) B.F. Fieselmann, D.N. Hendrickson, G.D. Stucky, *Inorg. Chem.* 17 (1978) 184;
(b) M.E. Lines, A.P. Ginsberg, R.L. Martin, R.C. Sherwood, *J. Chem. Phys.* 57 (1972) 1.
- [15] J.-P. Costes, F. Dahan, J.-P. Laurent, *Inorg. Chem.* 25 (1986) 413.
- [16] R.J. Butcher, C.J. O'Conner, E. Sinn, *Inorg. Chem.* 20 (1982) 537.
- [17] (a) M. Angaroni, G.A. Ardizzoia, T. Beringhelli, G.L. Monica, D. Gatteschi, N. Mascopchi, M. Moret, *J. Chem. Soc. Dalton Trans.* (1990) 3305;
(b) N.A. Bailey, D.E. Fenton, R. Moody, P.J. Scrimshire, E. Beloritzky, P.H. Fries, J.-M. Latour, *J. Chem. Soc. Dalton Trans.* (1988) 2817;
(c) F.B. Hulsbergen, R.W.M. Hoedt, G.C. Berschoor, J. Reedijk, A.L. Spek, *J. Chem. Soc. Dalton Trans.* (1983) 539.
- [18] O. Kahn (Ed.), *Magnetism: a Supramolecular Function*, Kluwer Academic Publishers, Boston, MA, 1996, pp. 159–164.